PHYSICAL REVIEW B **70**, 081307(R) (2004)

Excitation of radiative and evanescent defect modes in linear photonic crystal waveguides

M. Galli, M. Belotti,* D. Bajoni, M. Patrini, G. Guizzetti, D. Gerace, M. Agio, and L. C. Andreani
INFM and Dipartimento di Fisica "A. Volta," Università di Pavia, via Bassi 6, 27100 Pavia, Italy

Y. Chen
Laboratoire de Photonique et de Nanostructures, CNRS, Route de Nozay, 91460 Marcoussis, France
and Département de Chimie, Ecole Normale Supérieure, 24 Rue Lhomond, 75231 Paris Cedex 05, France
(Received 28 April 2004; published 26 August 2004)

The dispersion of line-defect modes in silicon-on-insulator photonic crystal waveguides is explored by means of angle- and polarization-resolved micro-reflectance measurements. The frequency-wave vector range accessible to the experiments is greatly expanded by the use of attenuated total reflectance, in addition to the standard one, thereby allowing one to study both truly guided (evanescent) and quasi-guided (radiative) photonic modes. The presence of a supercell repetition in the direction perpendicular to the line defect leads to the simultaneous excitation of defect and bulk modes folded in a reduced Brillouin zone. The group-velocity dispersion of defect modes corresponding to different polarizations of light is fully determined.

DOI: 10.1103/PhysRevB.70.081307 PACS number(s): 42.70.Qs, 42.82.Et, 78.20.Bh, 78.40.Fy

Periodically patterned planar waveguides, also known as photonic crystal (PhC) slabs, are emerging as one of the best performing structures for the control of light propagation in three dimensions (3D).[1–3] This is achieved by means of a two-dimensional (2D) photonic lattice combined with total internal reflection within the slab. Linear waveguides in PhC slabs introduce defect modes in the gap and support the propagation of light along the defect direction. A common system is realized in the triangular lattice of holes, by removing a row of holes along the Γ-K symmetry direction: this is called a W1 waveguide. The photonic dispersion may fall partly above the air light line in the k-ω plane, corresponding to the propagation of a quasi-guided photonic mode, and partly below the light line, giving rise to truly guided modes with very low losses.[4–6] The dispersion of defect modes is of crucial importance for physical properties and for applications, as it determines the propagation characteristics of light in the waveguide structure. Truly guided photonic modes exist only in PhC slabs with strong refractive index contrast between core and claddings, like the self-standing membrane or the silicon-on-insulator (SOI) system. These modes are evanescent in the direction perpendicular to the slab plane, and as such they are analogous to excitations in solids like surface plasmons[7] and surface polaritons.[8]

The dispersion of radiative modes in PhC slabs can be measured by angle-resolved reflectance or transmittance experiments from the crystal surface. The coupling between the incoming beam and photonic modes in the periodically patterned slab gives rise to resonant features in optical spectra, whose evolution as a function of incidence angle leads to a determination of the photonic band dispersion.[9–11] On the other hand, the dispersion of low-loss modes has been determined by resolving Fabry-Pérot fringes in waveguide transmission measurements on samples of specified length.[12,13] This technique has allowed the determination of the frequency dispersion of the fundamental (spatially even) defect mode in W1 waveguides realized on silicon membranes.[13]

In this work we show that the photonic mode dispersion across and below the light line can be probed by optical experiments from the crystal surface by means of attenuated total reflectance (ATR). The ATR technique is powerful for the study of surface excitations in solid-state systems,[7,8] yet it was never applied before to photonic crystals. Here the combined use of standard reflectance and ATR, both with high angular resolution and with polarization selection, leads to a determination of the photonic mode dispersion in an unprecedented frequency- and wave-vector range. We study SOI PhC slabs containing a W1 waveguide repeated with supercell periodicity. The frequency- and group-velocity dispersion of defect modes with both parities is determined in the radiative and guided-mode regions. Moreover, photonic modes of the periodic 2D system are folded into a reduced Brillouin zone by the supercell repetition and become observable. This phenomenon is the photonic analog of the folding of acoustic phonons in semiconductor superlattices, which makes them visible in optical spectra.[14]

Patterned waveguides containing W1 line-defects were fabricated by electron beam lithography and reactive ion etching techniques on smart cut SOI wafers having 0.26 -μm-thick Si core and 1-μm-thick SiO_2 cladding. A detailed description of the fabrication process is given in Ref. 15. W1 linear waveguides were realized in the triangular lattice of air holes with lattice constant $a=500$ nm and hole radius $r/a=0.34$. The patterned area of the samples was 300 $\times 300$ μm^2, and W1 line defects were repeated with different supercell periodicities $d=m\sqrt{3}a$ (with $m=4,5,6$) along the Γ-M direction. In the present work we focus on the sample with $m=5$, shown in Fig. 1(a).

Angle-resolved specular reflectance and ATR from the sample surface are measured in the spectral range 0.3–1.2 eV, at a spectral resolution of 0.5 meV, by means of a micro-reflectometer coupled to a Fourier-transform spectrometer (Bruker IFS66s). The angle of incidence θ is varied in the range $4°-75°$ with an angular resolution of 0.5° set by the very small but finite numerical aperture of the beam that is focused on the sample. Transverse-electric (TE) and transverse-magnetic (TM) polarizations with respect to the

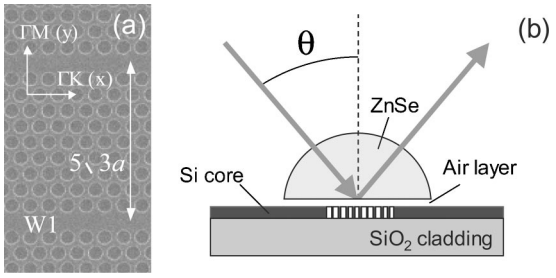

FIG. 1. (a) Scanning electron micrograph of the sample containing W1 line defects repeated with supercell periodicity $d=5\sqrt{3}a$ along the Γ-*M* direction; (b) Scheme of the experimental configuration for ATR measurements.

plane of incidence are selected by means of a KRS5 wire-grid polarizer.

The experimental geometry adopted for ATR measurements is shown in Fig. 1(b): a ZnSe hemisphere is brought close to sample surface at a very small separation (~250 nm). The thickness of the air layer between ZnSe and the sample determines the coupling strength of the incident light to the guided modes of the PhC slab, and is a critical parameter in the measurements. For this reason, the ZnSe hemisphere is kept in position over the sample surface by means of three piezoelectric actuators which allow fine tuning of the distance.

Experimentally determined photonic bands are compared with a full 3D calculation of the photonic dispersion, which consists of expanding the magnetic field on the basis of guided modes of an effective homogeneous waveguide. This method, which has been described elsewhere,[16,17] gives an accurate representation of the dispersion of guided and quasi-guided photonic modes. Reflectance spectra are calculated by the scattering-matrix method.[18] The extension to ATR spectra is straightforward, as it suffices to take the incoming beam in the prism material and to introduce an additional air layer between the prism and the patterned silicon layer.

In Fig. 2 we show the reflectance spectra of the sample for TE (a) and TM (c) polarized light measured along the Γ-*M* symmetry orientation, i.e., orthogonal to the W1 line defect.[19] The well-defined resonant features in the spectra are associated to the excitation of photonic modes of the patterned waveguide. While resonances corresponding to bulk modes are characterized by a strong dispersion as a function of the incidence angle, the defect modes are clearly observable as dispersionless resonances occurring at 0.73 and 0.89 eV for TE and TM polarizations, respectively. Very good agreement is found by comparing the photonic bands extracted from experimental data to the theoretical ones, as shown in Figs. 2(b) and 2(d). Notice that photonic bands are folded into a reduced Brillouin zone $[-\pi/d, \pi/d]$ due to supercell repetition along the Γ-*M* direction. This also causes the fundamental guided mode of the bulk 2D system to become observable in a reflectance measurement and to form small gaps at the zone center and edges: in particular, minigaps up to ~0.01 eV are observed in the experiment and reproduced in the theory.

The polarized reflectance spectra measured for light incident along the Γ-*K* orientation are shown in Figs. 3(a) and

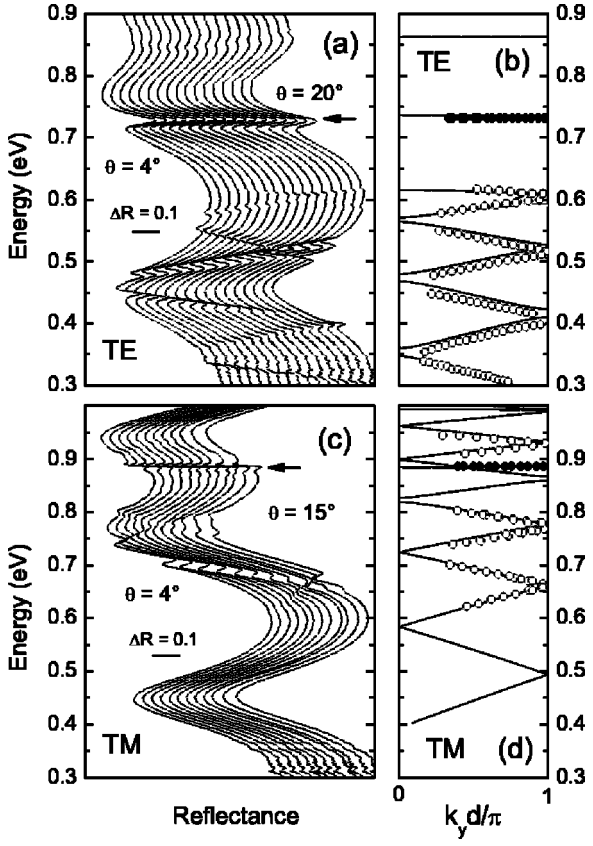

FIG. 2. (a),(c) Reflectance measurements along the Γ-*M* orientation for TE and TM polarizations on the sample of Fig. 1(a). The curves are slightly shifted for clarity. The defect modes are indicated by arrows. (c),(d) Corresponding photonic bands folded into a reduced Brillouin zone due to supercell periodicity: experiment (closed circles for defect modes, open circles for bulk modes) and theory (lines).

3(c).[19] Also in this case the spectra display several resonances which mark the excitation of photonic modes. However, since we are now measuring in the direction parallel to the W1 waveguide, the defect modes exhibit a dispersive character due to propagation along the channel. The calculated reflectance spectra [shown in Fig. 4(a) for TE polarization] show a very good agreement with the experimental data. In Figs. 3(b) and 3(d) the attenuated total reflectance measurements are reported. Only a selected range of angles corresponding to states below the light line of SiO_2 (truly guided region) are shown. The angle- and polarization-resolved ATR spectra look very different from the reflectance ones. They are characterized by strong, "absorption-like" dips superimposed on a constant value very close to unity (the total reflection region). While the resonances in reflectance spectra have absolute amplitudes of the order of 0.05, those appearing in ATR can reach amplitudes up to 0.8. Such a highly efficient energy transfer process is due to the excitation of evanescent modes in the waveguide for proper overlapping of the exponentially decaying fields at the ZnSe-air-sample interface. The ATR resonances are particularly prominent because of the constant background (unlike for reflectance in the radiative region). Evanescent (truly-guided) modes lying below the light line should in principle

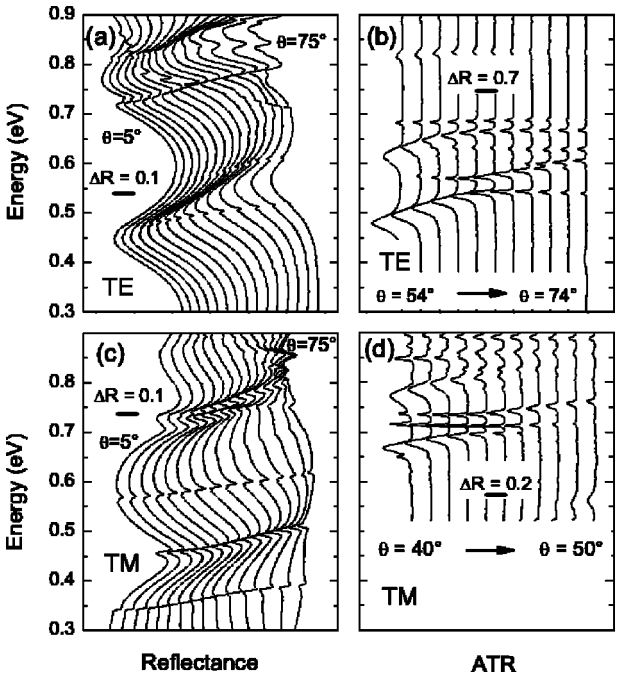

FIG. 3. Experimental reflectance (a),(b) and ATR (c),(d) measured along the Γ-*K* orientation, for TE (a),(c) and TM (b),(d) polarizations. Curves are shifted for clarity.

have zero losses and therefore a vanishing linewidth. On the other hand, the line shapes observed in ATR exhibit a finite width depending on the separation distance between the ZnSe hemisphere and the sample. For very small values of the distance, the guided modes are severely affected by the presence of the hemisphere, and we observe strong coupling with large linewidths and energy shifts of the modes. As ZnSe is separated from the sample, the resonances become sharper and do not show any shift in energy. We notice that the optimal air-layer thickness depends on the energy and on the angle of incidence: here the separation distance has been optimized for the detection of defect modes, and for TM polarization it has been found to be about twice that for TE polarization. In order to better elucidate the effect of prism-induced width of the evanescent modes, the measured spectra were compared to calculated ATR for different air-layer thicknesses. By setting the separation between ZnSe and the sample at 250 nm, as in Figs. 4(b), a surprisingly good correspondence for both energy positions and line shapes of the resonances is observed.

By combining results obtained from reflectance and ATR measurements, the photonic band dispersion of the PhC waveguide along the Γ-*K* direction can be traced. This is shown in Figs. 5(a) and 5(b), where the dispersion extracted from experiments is compared to calculations for TE and TM polarizations, respectively.[19] As a first remark, we notice that many modes are observed experimentally (and accounted for theoretically) as compared with the band diagram expected for the simple 2D triangular lattice. These are photonic modes of the 2D bulk system which are discretized and folded in a reduced Brillouin zone due to supercell repetition of the line defect in the Γ-*M* direction. There is a very good agreement between measured and calculated dispersion, both

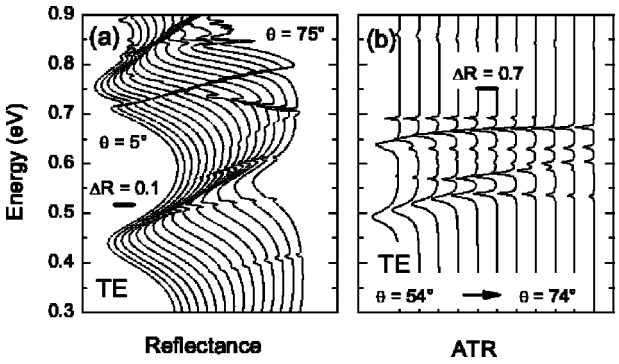

FIG. 4. Calculated reflectance (a) and ATR (b) spectra along the Γ-*K* orientation, for TE polarization. The ATR calculation in (b) assumes an air-layer thickness of 250 nm.

for radiative and evanescent modes;[20] the small (<0.008 eV) remaining discrepancies are attributed to the frequency dispersion of the Si dielectric function (not included in the calculations). Due to the high *k*-values attainable by ATR measurements, many of the experimental points correspond to wave vectors that fall outside the first Brillouin zone, and are therefore folded back. This yields a fine mesh in the experimentally determined dispersion which allows one to reproduce the details of photonic states in the most interesting region close to the zone edge. The defect modes can be distinguished from bulk modes by a comparison with the photonic bands measured along the Γ-*M* orientation (Fig. 2), which yields the energies of the modes at the Γ point. A somewhat surprising result is that the polarization character of the defect modes changes on turning from the Γ-*M* to the Γ-*K* orientation: this behavior corresponds to a change of the mirror plane of the photonic crystal structure and reflects the microscopic symmetries of the defect modes.

Considering now the defect dispersion across and below the light line, we observe that the TE-polarized defect mode is characterized by a pronounced dispersion in the radiative region which becomes very flat in the guided region, where the mode propagates with low group velocity.[13] On the other hand, the TM-polarized defect mode exhibits the opposite behavior, being weakly dispersive in the leaky region and more dispersive in the guided region. In Fig. 6 we plot the group velocities of the defect modes as obtained directly from the derivative of the measured dispersion. The highly dispersive nature of the TE-polarized defect is evidenced by the very fast change in group velocity, which is dramatically reduced while crossing the air light-line, and reaches the very small value $\sim c/100$ in the guided region. A completely different behavior is observed for the TM-polarized mode, whose group velocity starts with positive values in the leaky region, then vanishes at the light line and becomes negative in the guided region. Such unique dispersion characteristics are substantially different as compared to conventional waveguides and photonic crystal fibers, and are peculiar to the photonic confinement achieved in W1 line defects. This should add to the various known examples of surface-mode dispersion in solid-state systems.[7,8]

The photonic band dispersion of linear photonic crystal waveguides has been determined by the combined use of

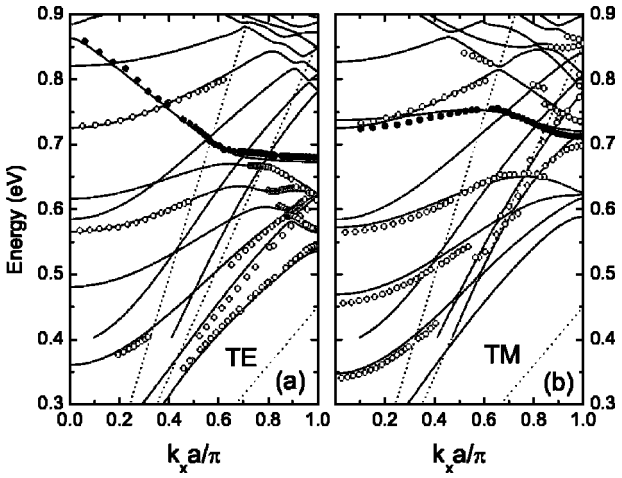

FIG. 5. Measured dispersion of the photonic bands as derived from reflectance and ATR (closed circles for defect modes, open circles for bulk modes), compared to calculated dispersion (lines). Dotted lines: light lines of air, SiO_2 and Si.

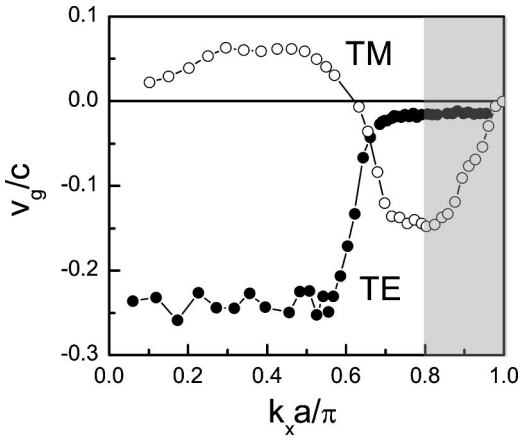

FIG. 6. Group velocity of the defect modes for TE and TM polarizations. Shaded area indicates the truly guided region.

angle- and polarization-resolved reflectance and ATR. The distinction between defect and bulk modes is provided by measurements in directions parallel and perpendicular to the defect axis. A comparison with calculated bands and spectra shows that the mode dispersion in the radiative and guided regions is understood even in fine details. This is of particular importance for the defect modes whose group velocity must be controlled to a high degree of accuracy. The ATR technique proves to be very powerful for the study of dispersion properties in PhC slabs supporting guided photonic modes.

This work was supported by MIUR through Cofin and FIRB programs.

*Also at LPN-CNRS, 91460 Marcoussis, France.

[1] K. Sakoda, *Optical Properties of Photonic Crystals* (Springer, Berlin, 2001).

[2] See papers in IEEE J. Quantum Electron. **38**. Feature section on photonic crystal structures and applications, edited by T. F. Krauss and T. Baba, pp. 724–963 (2002).

[3] S. G. Johnson and J. D. Joannopoulos, *Photonic Crystals: the Road from Theory to Practice* (Kluwer, Dordrecht, 2002).

[4] T. Baba, A. Motegi, T. Iwai, N. Fukaya, Y. Watanabe, and A. Sakai, in Ref. 2, p. 743.

[5] M. Notomi, A. Shinya, K. Yamada, J. Takahashi, C. Takahashi, and Y. Yokohama, in Ref. 2, p. 736.

[6] S. McNab, N. Moll, and Y. Vlasov, Opt. Express **11**, 2927 (2003).

[7] H. Raether, *Surface Plasmons* (Springer, Berlin, 1988).

[8] *Surface Polaritons*, edited by V. M. Agranovich and D. L. Mills (North-Holland, Amsterdam, 1982).

[9] T. Fujita, Y. Sato, T. Kuitani, and T. Ishihara, Phys. Rev. B **57**, 12 428 (1998).

[10] V. N. Astratov, D. M. Whittaker, I. S. Culshaw, R. M. Stevenson, M. S. Skolnick, T. F. Krauss, and R. M. De La Rue, Phys. Rev. B **60**, R16 255 (1999).

[11] A. D. Bristow, D. M. Whittaker, V. N. Astratov, M. S. Skolnick, A. Tahraoui, T. F. Krauss, M. P. Croucher, and G. A. Gehring, Phys. Rev. B **68**, 033303 (2003).

[12] D. Labilloy, H. Benisty, C. Weisbuch, C. J.M. Smith, T. F. Krauss, R. Houdré, and U. Oesterle, Phys. Rev. B **59**, 1649 (1999).

[13] M. Notomi, K. Yamada, A. Shinya, J. Takahashi, C. Takahashi, and I. Yokohama, Phys. Rev. Lett. **87**, 253902 (2001).

[14] P. Y. Yu and M. Cardona, *Fundamentals of Semiconductors* (Springer, Berlin, 1996), p. 496.

[15] D. Peyrade, Y. Chen, A. Talneau, M. Patrini, M. Galli, F. Marabelli, M. Agio, L. C. Andreani, E. Silberstein, and P. Lalanne, Microelectron. Eng. **61-62**, 529 (2002).

[16] L. C. Andreani and M. Agio, in Ref. 2, p. 891.

[17] L. C. Andreani and M. Agio, Appl. Phys. Lett. **82**, 2011 (2003).

[18] D. M. Whittaker and I. S. Culshaw, Phys. Rev. B **60**, 2610 (1999).

[19] We emphasize that TE- (TM-) polarized photonic modes are defined with respect to the plane of incidence shown in Fig. 1(b), which depends on the orientation of the incident beam with respect to the photonic structure. In the calculations, these modes are defined to be odd (even) with respect to a vertical mirror plane: this overall symmetry takes into account both spatial parity and the transformation properties of the field components.

[20] Only prominent structures that could be definitely assigned to photonic modes are reported in Fig. 5. The fact that the lowest TM bands are not clearly visible in the spectra may follow from the larger extension of the TM waveguide mode, which requires a larger separation distance of the ZnSe prism, and to the choice of optimizing the distance for observation of the defect modes.